Controls on Pollution Ozone Production Measurable from Surface, Aircraft, and Satellite Monitors

Robert B. Chatfield[1], Xinrong Ren[2], William H. Brune[3], James H. Crawford[4], Robert Esswein[5,1], Alan Fried[6], Jennifer R. Olson[4], Richard E. Shetter[6]

Widespread airborne sampling of HO_2 and more broadly measurable species over North America suggests empirical measures of regional ozone production. Two variables are important: the well-known ν = [NO], and $\phi = j_{HCHO}$ [HCHO], a gauge of organic oxidation rate. Ozone production functions as a semi-parametric fit $F_2(\phi,\nu)$, or a more theoretically based $Q_2(\phi,\nu)$, serve in different contexts. F_2 and Q_2 both give traditional empirical kinetic model assessment (EKMA) insights a measurable, local expression, and help define control strategies. At low $\phi \bullet \nu$, O_3 production is described as $f_1(\phi \bullet \nu)$, starting linear and dropping to sub-linear. We expect that similar ϕ,ν analysis may help separate O_3 transport from photochemistry, providing a language to express generalizations about complex kinetic systems and observations. We suggest: (i) a network of moderate-technology rural sampling stations; (ii) more broadly, analysis derived from remote sensing, mapping near-surface j_{HCHO}, HCHO and NO_2 (related to NO).

1. Dissecting Subcontinental Smog Ozone Production and Control

NASA's investigation of air pollution over the Eastern North America and its outflow into the Atlantic provided a remarkably broad sample of the polluted atmosphere during a moderate-pollution summer, July–August, 2004. Measurements made aboard the DC-8 flying laboratory during the INTEX-NA studies within ICARTT [Singh et al., 2007, Ren et al., 2008] yielded relationships utilizing measurements of only HCHO, NO, and UV that describe the chemical production rate of smog ozone with useful accuracy. Such formulas deserve further testing and application since the abatement of smog ozone has substantial economic value: health and crop productivity concerns must be related to the costs of restricting emission of ozone precursors from a wide variety of sources which may be kilometers or thousands of kilometers upwind. [NAAMS Draft, 2005, Solomon, Seinfeld, 1998, Jacobson, 1998, McKeen et al., 1991] For both forecasting and control, local ozone production must be distinguished from transported ozone [NAAMS Draft, 2005, Chatfield and Delany, 1990, McKeen et al., 1991, Sillman et al., 2002]. It is highly desirable to have broad maps of such indicators for the ozone production process. Space-borne observations could give broad and informative maps.

Gross production of tropospheric ozone P_{O_3}, according to established theory, can be written the consequence of either of two peroxy radical reactions [Seinfeld and Pandis, 1998, Jacobson, 1998], contributing to a broader class of chemically interchanging oxidants (NO_2, NO, O_3) whose predominant species is ozone:

$$HO_2 + NO \rightarrow OH + NO_2$$

or $$ROO + NO \rightarrow RO + NO_2$$

$$\ldots NO_2 + h\nu \rightarrow NO + O$$

$$\ldots O + O_2 \rightarrow O_3$$

and the rate is determined by $P_{O_3} = k_H[HO_2][NO] + k_R \Sigma_i [ROO]_i [NO]$, omitting very minor pathways. Here, ROO stands for one of many organic radicals with a C-O-O peroxy structure. We call P_{O_3} directly computed, but admit, in fact, there are implicit model assumptions about reaction rates and products. (E.g., the rate k_R describes reactions producing not peroxynitrates but NO_2 ; relative yields may have uncertainties.) As we shall see, the HO_2 reaction usually contributes 50–70% of P_{O_3}, depending somewhat on H/C ratio and structure of the smoggy volatile organic compound (VOC) mix. Consequently we refer to $P^{\circ}_{O_3} = k_H[HO_2][NO]$ as the "principal ozone production rate," a rate unambiguously measured. The residual ($P_{O_3} - P^{\circ}_{O_3}$) due to ROO radicals is intrinsically highly correlated to $P^{\circ}_{O_3}$ since reactions producing ROO's involve the creation of HO_2's and vice versa [Seinfeld and Pandis, 1998, Jacobson, 1998, Saunders et al., 2003]. The creation of ROO's and HO_2's involves complex smog chemistry extending to tens of thousands of reactions; rate coefficients for these must be estimated from limited data, as must the yield when more than one product is possible. Consequently, measures of $P^{\circ}_{O_3}$ may provide useful analytical tools and guidance. (While chemical loss and deposition of O3 can pose difficulties in certain important situations [Carroll et al., 2001], they are separable and beyond the current analysis.)

Some previous empirical analyses on airmass ozone production, emphasizing P_{O_3} and $P^{\circ}_{O_3}$ chemical production have utilized coordinate production of other oxidation products such as HNO_3 and H_2O_2, while admitting that inferences are influenced by rapid and perhaps sporadic dry and wet removal of these species [Sillman et al., 2002]. In any case these usefully emphasize the entire history of chemical ozone net production from a major emission event (e.g., an urban or regional plume) rather than a local view more appropriate to the formulation of more localized control measures. Thornton et al. [2002] make a local analysis employing a full suite of instrumentation. Kleinman's [Kleinman, 2005a, Kleinman et al., 2005b] analyses employ kinetic simulations of VOC/NO_x mixtures; nevertheless the themes and analyses are ones that this work emulates. The twin complexities of complex reaction pathways and difficult-to-simulate transport argue for broad space-borne observations augmented by widespread, if scattered, rural observations.

Frequent measurements on the DC-8 of boundary layer HO_2, NO, and other variables allowed this principal ozone production rate to be calculated. The rich variety of measurements made on board [Singh et al., 2007] also allowed an approximate estimation of the ROO radicals through chemical simulations [Olson et al., 2001]. Significantly, we find that ozone production estimated with high-technology radical measurements can be approximated well with less demanding, expensive instruments measuring just two smog precursors. Nearly a thousand smoggy boundary-layer mixtures were measured below 1300 m and extended from Texas to Ontario to Boston to Atlanta, and into the Western Atlantic (see Supplemental Material).

We begin by highlighting two important controlling dimensions: first, ν = [NO], the easily measured component of NO_x which which is well know for its role in converting peroxies to ozone; then, second $\phi = j_{HCHO}$ [HCHO]. We associate ϕ with the reactive flux of organic species that simulaneously create and destroy formaldehyde while producing peroxy

radicals; the crux of this work is to initiate study of the degree of useful guidance which ϕ provides. The abstract names ϕ and ν and are meant to suggest a decomposition of the smog production problem into a peroxy-determining reaction-flux of VOC and an efficiency of conversion of the peroxies to ozone. ϕ is thought important not just because HCHO photolysis is an important source or radicals itself, even though as much as 25–30% of ther radicals originate from HCHO reactions in one urban study [Lee et al., 1998]. Rather ϕ embodies many correlations with the HO_2-producing activity depending on the action of hard UV on organics which are more difficult to measure. HCHO is common at the end of known VOC oxidation chains. Glyoxal and methyl glyoxal should be lesser rivals as end-products and indicators, mostly for mixtures rich in lower H/C ratio species [Saunders et al., 2003 and work referenced there]. Extended work employing glyoxal and photolysis rates similarly cannot be explored here. The j_{HCHO} [HCHO] indicator may also usefully parallel other radical production pathways involving, e.g., O_3 photolysis producing OH and other VOC reactions. At the simplest level, it converts HCHO measurements to one VOC-processing rate; counterbalancing sources and sinks can leave substantial quantities of HCHO in low-radical situations, e.g. at night.

2. Interpreting Interactions of Radical-Producing and Radical-Converting Variables

Figure 1a provides a contour plot of an emprically estimated function F_2, allowing independent fitting to many combinations of variables ϕ and ν = [NO]. The supplement describes the estimation; variance explained was ~82%. When F_2 is plotted on linear axes (Figure 1a), the shape of the contours is similar to the "EKMA" Empirical Kinetic Modeling Approach method used to address a similar O_3 problem: EKMA related morningtime [NO_x] and VOC concentrations to O_3 produced 6-8 hours later, ignoring transport. The method improved over previous "linear rollback" abatement strategies since it recongized complex VOC/NO_x interaction and the sub-linearity of ozone production; however, it was eclipsed by three-dimensional transport models [Shafer and Seinfeld, 1985, U.S. EPA, 1987]. F_2 is by contrast a local measure, approximately defined by a distance scale that recognizes a 1-3 hour middle-of-the-day turnover time of HCHO. It lacks features of EKMA, most notably a large triangular "notch" of low ozone in the upper left hand corner of EKMA plots. High morning-time NO primarily lowered later O_3 by the need for NO+O_3 to react to NO_2; other multi-hour effects (e.g., the OH+NO_2 reaction eventually lowering NO_x) also contribute somewhat. We believe that F_2 builds on the analyses of Kleinman for nearer-source descriptions of VOC and NO effects based on measurable VOC's, and also of Martin, using satellite analyses of boundary layer NO_2 and HCHO to suggest somewhat more quantitatively broad-area VOC vs NO_x control [Martin et al., 2004]. The greatest reduction in ozone production is achieved by moving downwards perpendicular to the contour lines; of course, tonnage-restriction of NO and tonnage removal of VOC's that reduce ϕ may have different costs and imply a different strategy.

Figure 1a suggests that F_2 contours are nearly simple contours of $\phi \bullet \nu = constant$. An F_2 plot using logarithmic scales in Figure 1b shows this near-hyperbolic behavior more cleanly, and emphasizes the strong role of a single variable, $a = \phi \bullet \nu$. Departures from this behavior

(e.g., additional VOC effects) are indicated by deviations from lines such as the dashed red lines in Figure1a and Figure 1b. Control strategies implied by the log-log plots are slightly different from the linear plot: to move straight downwards (most effective control), *proportional* reductions are implied, not equal-tonnage reductions in emissions.

These observations naturally suggested that an even simpler representation of $P^{\circ}_{O_3}$ was available as an f_1 ($\phi \bullet \nu$), that is f_1 (j_{HCHO} [HCHO] [NO]). This was determined by a spline fit emphasizing simplicity; f_1 is shown in Figure 2a; it also emphasizes the less-than-linear production of at high $\phi \bullet \nu$ in Figure 1a. This is a major feature resembling the EKMA description. We present the relationship as *statistically* justified [Venables and Ripley, 2004] over a very large diverse sample of smog ozone production rates of less than ~4 ppb hr^{-1}, and, suggest further validation in more varied circumstances.

The f_1 relationship is simply a more complete quantification of earlier understandings emphasizing the roles of NO and UV radiation [Haagen-Smit, 1952, Leighton, 1961, Lin et al. 1988, Liu et al. 1987]. We can quantify the advance of understanding: Whenwe estimated with similar procedurees a the sequence of best estimates using progressively more information, which we will label f_0 ([NO]), f_{00} (j_{HCHO} [NO]) and f_1 (j_{HCHO} [HCHO] [NO]) the variance explained rose sharply: <50–60%, <63–69% and 79%. f_0 ([NO]), f_{00}(j_{HCHO} [NO]) also suggest even more complex functional behavior at values of $\phi \bullet \nu$ higher than 0.25 ppb^2/hr. Kleinman [2005a] describes a power law based on those VOC's which can be measured (see Supplement).

We would expect the HCHO-based relationships to become applicable over time periods of 1–3 hours corresponding to its midday lifetime, as VOC oxidation and NO_x effects adjust. There needs be time for any fresh NO to come into the Leighton [1961] quasi-steady state with O_3 and NO_2, at least ~300 seconds from mid-morning to mid-afternoon. More stringently, HCHO needs to come into a quasi-steady state with its source and product compounds, typically ~2 hours around midday, but ~12 hours at dawn or dusk. Additionally, strong sources of freshly emitted VOC and HCHO mixtures may need to adjust to build HCHO from VOC's or consume primary HCHO.)

3. Comparison to More Theoretically Based Methods

A somewhat more theoretical description of ozone production informing these statistical results is available by equating the production and loss rates of the transient HO_2 radical. The quasi-steady-state approximation for HO_2 suggests that

$$2\eta k_{HH} [HO_2]^2 + (1-\rho) k_{NH} [NO] [HO_2] = \gamma j_{HCHO} [HCHO]$$

The supplement describes the kinetic rate coefficients and some additional parameters (η,ρ, and γ), parameters necessary to address some complexities contributed by statitistically correlated reactions directly affecting HO_2. Briefly, γ summarizes related HO_2 (new HO_x) production pathways, η summarizes peroxy-peroxy destruction reactions strongly correlated to HO_2+ HO_2, and ρ summarizes radical recycling producing HO_2 as some fraction of the HO_2+NO destruction reaction. Each parameter was necessary to produce reasonable graphs of HO_2 as a function of NO [Ren et al., 2008] although the set (η,ρ, and γ) clearly exhibts one

linear dependency: production and destruction rates of HO_2 can offset each other and still yield the same solution. This is a two-parameter fit which is limited to the same observable Quantities. Solving the quadratc to obtain HO_2 and thus the ozone production rate, we have

$$P^{\circ}_{O_3} = Q_2(\phi,\nu) = k_{NH}\gamma\left(j_{rads}[HCHO][NO]\right)\Big/\left[(1-\rho)k_{NH}[NO] - \sqrt{(1-\rho)^2 k_{NH}{}^2[NO]^2 + 4k_{NH}\gamma\, j_{rads}[HCHO]}\right]$$

The fundamental role of $\phi \bullet \nu$ is clear from the numerator, and so is a degree of less-than-linear response indicated by f_1 as both radical production ϕ and ν increase in progressively more polluted situations. The form of the response behavior at higher $\phi \bullet \nu$ is less clear, as is the approximate $\alpha^{0.4}$ behavior at values of $\phi \bullet \nu$ higher than 0.05 in Figure 2a. Figure 3a shows that ozone production using this formula with observed data displays much the same form as f_1. This two-parameter fit exhibits a lower r^2, 0.75, vs. 0.79 for the completely empririal plots. f_1 and F_2 appear more successful than Q_2 for low-VOC, high NO situations, reflecting observed HO_2 behavior that is not fully understood [Ren et al., 2008]. Why do the empirical relationships emphasize higher $P^{\circ}_{O_3}$ at low ν/ high ϕ and even more strongly at high ν/ low ϕ? Are there actually variations in ρ or η? The quadratic method may deserve elaboration with broader datasets. Analyses of the family HO_x = HO_2+ OH could address these questions [Thornton et al., 2002], but we found no way to describe HO_x with just a few simple measurements.

In order to complete the description of ozone production, some estimate of the relationship of total production P_{O_3} to $P^{\circ}_{O_3}$ is required. While measures of total ROO+HO_2 radicals are steadily being improved, their interpretation goes beyond this brief report. Mechanisms of photochemical reaction based on laboratory measurements can be used to relate these quantities; two methods are available. One is the use of complete three-dimensional models with carefully checked emissions of organics. While useful, errors in transport and emissions as well as necessarily limited chemical mechanisms can affect results. "Point" models as employed are closely tied to the observations made on the DC-8 but must approximate complex chemical history with a simple diurnally repeating steady state [Olson et al., 2001. Limited VOC measurements also restrict the number of cases to ~280, suggesting point-model effects are more approximate. We found for this dataset that P_{O_3} = 1.6 x $P^{\circ}_{O_3}$, as shown in Figure 2b. This ratio is expected to vary somewhat, between 1.3 and 2, with the chemical composition of the reacting VOC mixture; most basically high C/H ratios in the VOC favor a higher ratio. In Figure 3b, contour plots based on the point-model calculations of ϕ and ν appear roughly intermediate between the Q_2 and F_2 contour plots, suggesting methods to critique each.

4. Conclusions: Extend Sampling to Rural Sites and to Space

Simulations with organic reaction mechanisms for various compounds suggest that there should be variations for (a) different organic mixes, some making for higher j_{HCHO} [HCHO], some making for less, and that (b) HCHO may not be exactly in an evolving "quasi steady state" so that j_{HCHO} [HCHO] uniformly represents peroxy radical levels (HCHO may be increasing or decreasing significantly enough to affect the analysis). Both of these situations will occur closer to pollution sources, which are more likely to have idiosyncratic compositions

(e.g., refinery emissions, aromatic emissions, …) and also to be highly reactive and transient. The widespread rural relationship described by our samples may not apply with the very same parameters. Still, the relationships might be broadened to allow insights and methods which separate HCHO-to-radical relationships from broader effects describing the intensity and the NO_x-sensitivity of VOC oxidation activity, as suggested by forms like F_2, Q_2, and f_1.

The results we analyze from widespread extra-urban sampling seem to suggest that the formaldehyde oxidation rate (j_{HCHO} [HCHO]) is particularly able to define the oxidation rate of all organics (more exactly, the concentrations of peroxy and organic-peroxy radicals). We suggest study of the usefulness of this technique in at least two directions. One is to make widespread characterizations of rural sites so as to describe regional smog, describing unsuspected ozone production hotspot situations and their VOC or NO_x sensitivity. Step-by-step, measurements and analysis can approach nearer-source air chemistry. The approach can also be used for a three-dimensional model improvement tool, validating the calculation of [HO_2] and consequently [ROO]. The general description of ozone chemical production rate can be used to highlight and define situations in which such models (e.g., the Community Model for Air Quality) may overestimate, or possibly miss important peroxy radical sources. We have initiated analyses in situations in which [HO_2] was measured, and find it useful; however sites and situations away from strong sources and sinks (NO emissions, deposition, etc) are preferred. Rural, tall-tower measurements should be most informative about regional chemistry, even plume chemistry.

Finally, components defining ϕ and ν, lowermost-troposphere HCHO, NO_2 and UV radiation are currently measured with satellite technology. It will be helpful to create a very empirical description of ozone production, using these variables, and deducing NO from NO_2 and lower-tropospheric O_3. We do not elaborate, but note that this builds on current work [Martin et al., 2004]. With modest investment, capabilities for lowermost troposphere HCHO and O_3 measurements may steadily improve, for example with new technology exploiting the 3-μm region; boundary layer remains the most difficult observation [Kumer et al., 2006]. More quantitatively, the maps of integrated-column j_{HCHO} [HCHO] and NO_2 variables can closely constrain three-dimensionsal simulation models. Maps of f_1, F_2 , or Q_2, can specify regions most deserving of improvement in emissions or simulation. Remote sensing measurements can then constrain both the NO availability and the HO_2 production rates in studies using complex three-dimensional models. Because the information we have added to prior knowledge refers to organic radical reactivity and especially peroxy radicals, we have nick-named the method "POGO-FAN," Production of Ozone by Gauging of (organic) Oxidation – Formaldehyde Activity and Nitric oxide. The name recognizes, in an American idiom, a collective responsibility to limit ozone pollution for our own good.

Acknowldegements: "We have met the enemy and he is us," as recognized by Walt Kelly's cartoon figure Pogo. We thank the American Chemical Council for sponsorship initiating this study, and the NASA Tropospheric Chemistry program for the main data and research support. Hanwant B. Singh, Laura Iraci, and Sanford Sillman made useful suggestions.

References:

Carroll, M.A., S. B. Bertman, P. B. Shepson, Overview of the Program for Research on Oxidants: PHotochemistry, Emissions, and Transport (PROPHET) summer 1998 measurements intensive, *J. Geophys. Res.*, *106*(D20), 24,275–24,288, 2001.

Haagen-Smit, A.J., Chemistry and physiology of Los Angeles smog. *Ind. Eng. Chem. 44, 1362,* 1952.

M. Jacobson, *Fundamentals of Atmospheric Modeling,* (Cambridge U. Press, Cambridge, 1998).

Kleinman, L.I., The dependence of tropospheric ozone production rate on ozone precursors, *Atmospheric Environment* **39** (2005), pp. 575–586, 2005a

Kleinman, L.I., et al, A comparative stduy of ozone production in five U.S. metropolitan areas, *J. Geophys. Res., 110,* doi:10.1029/2004JD005096 2005b.

Kumer, J. et al., Tropospheric infrared mapping spectrometers (TIMS) for air quality measurements, Tropospheric infrared mapping spectrometers (TIMS) for Air Quality measurements, *Proceedings of the SPIE, 6299*, pp. 629908 (2006)

Leighton, P.A., *Photochemistry of Air Pollution, (*Academic, Press, San Diego, Calif., 1961*).*

Lin, X., M. Trainer, S. C. Liu, On the nonlinearity of tropospheric ozone production,*J. Geophys. Res., 93,* 15,879-15,888 ,1988.

Liu, S.C. M. Trainer, F. C. Fehsenfeld, D. D. Parrish, E. J. Williams, D.W. Fahey, G. Hubler, P.C. Murphy, *J. Geophys. Res., 92,* 4191 (1987).

Martin, R.V., A. Fiore, A Van Donkelaar, *Geophys. Res. Lett., 31,* L06120, doi:10.1029/2004GL019416, 2004.

McKeen, S.A., E.-Y. Hsie, S. C. Liu (1991), *J. Geophys. Res.*, *96*, 15,377 (1991).

NAAMS Draft, *Draft National Ambient Air Monitory Strategy,* Office of Air Quality Planning and Standards, Research Triangle Park, NC, December, 2005.

Olson, J.R., et al., *J. Geophys. Res.*, *106*(D23), 32,749–32,766 (2001).

S. M., Saunders, M. E Jenkin,. R.G. Derwent, M.J. Pilling, Protocol for the development of the Master Chemical Mechanism, MCM v3 (Part A): tropospheric degradation of non-aromatic volatile organic compoundsAtmospheric Chemistry and Physics, 3, 161-180, 2003.

Ren, X., J. R. Olson, J. H. Crawford, W. H. Brune, J. Mao, R. B. Long, Z. Chen, G. Chen, M. A. Avery, G. W. Sachse, J. D. Barrick, G. S. Diskin, L. G. Huey, A. Fried, R. C. Cohen, B. Heikes, P. O. Wennberg, H. B. Singh, D. R. Blake, R. E. Shetter, HOx Chemistry during INTEX-A 2004: Observation, model comparison and comparison with previous studies, *J. Geophys. Res.*, 113, D05310, doi:10.1029/2007JD009166, 2008

Shafer, J. T.. J. Seinfeld, *Evaluation of Chemical Reaction Mechanisms for Photochemical Smog. Part 3. Sensitivity of EKMA (Empirical Kinetic Modeling Approach) to Chemical Mechanism and Input Parameters,* U.S. Environmental Protection Agency, Washington, D.C., EPA/600/3-85/042 (NTIS PB85210888, 1985).

Seinfeld, J.H., and S.N. Pandis, *Atmospheric Chemistry and Physics* (J. Wiley, Hoboken (1998).

Sillman, S., D. He, *J. Geophys. Res.107, 10.1029/2001JD001123, 2002.*

Singh, H. B., et al., *J. Geophys. Res.*, *112*, doi:10.1029/2006JD007664 (2007).

Solomon, *Atmospheric Environment 34,* 1885(2000).

Ren, X., et al., *J. Geophys. Res.*, *in press,* 2008.

Thornton, J.A. et al., *J. Geophys. Res.*, *107*, 4146, doi:10.1029/2001JD000932 (2002).W.N.

U.S. EPA, U.S. EPA, *Guidelines of Use of the City-Specific EKMA in Preparing Post-1987 SIP'S* , Office of Air Quality Planning and Standards, Research Triangle Park, North Carolina, 1987.

Venables, W.N. B.D. Ripley, *Modern Applied Statistics with S,* (Springer Verlag, New York, 2004), pp 38–243.

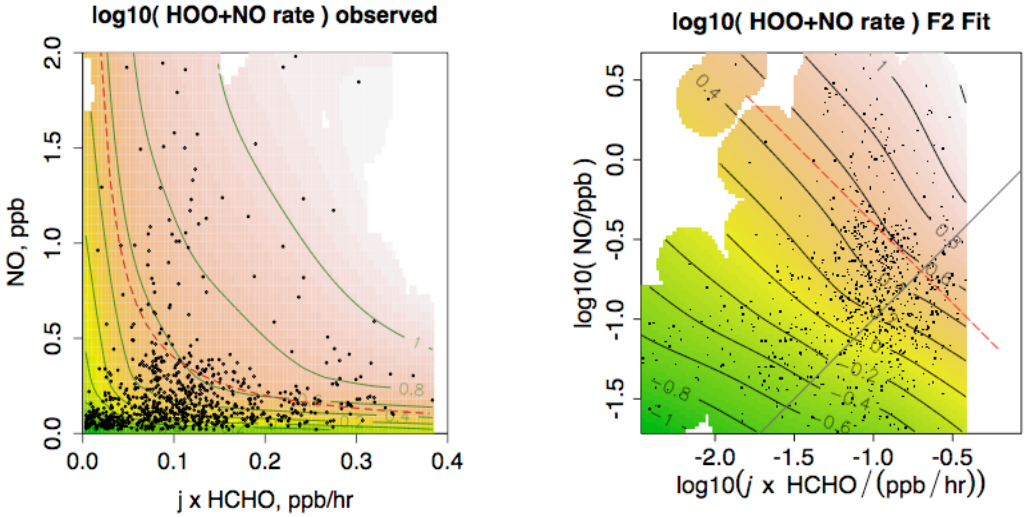

A **B**

Fig. 1. (a) Statistical-fit F_2 of principal production rate of ozone $P^{\circ}_{O_3}$ as a function of the product (j_{HCHO} [HCHO] and of [NO] with datapoints shown. Large variations of ozone production are shown as contours of log ($P^{\circ}_{O_3}$ / (ppb/day)). (b) Logarithmic axes are employed for the same information in second panel. 1:1 line shown. Red hyperbola and 1:1 and 1:-1 (slope) straight lines help define isopleths of $\phi \bullet \nu$. Most effective control strategies for O_3 for any particular mix at any data point are downward normals to the contours shown.

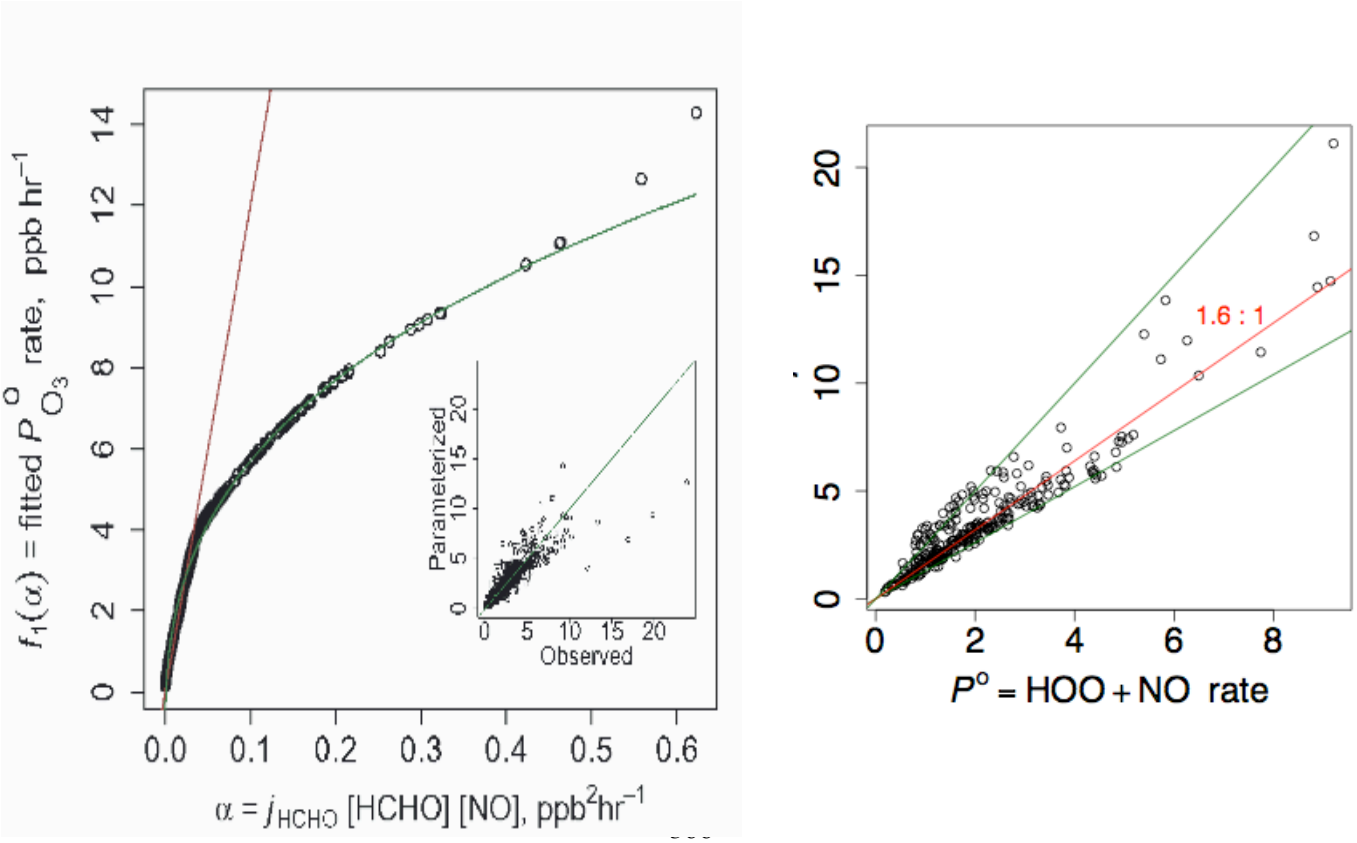

307

Fig. 2. Statistical-fit f_1 of principal production rate of ozone $P^{o}_{O_3}$ as a function of the product $\alpha = \phi \bullet \nu = j_{HCHO}$ [HCHO] [NO] which summarizes several smog processes. Small circles show individual data instances with modeled response; line shows interpolation and extrapolation of the fit. Inset shows correlation of the fit with direct computations of $P^{o}_{O_3}$ using measurements made in INTEX-A flights over much of North America. Approximating red line has slopes of 120 and the green curve is the approximation 16 $\alpha^{0.37}$–1.3. Correlation plot is inset. Correlation is 0.88, but rises to 0.91 if one high and four low points are dropped. (b) Relationship of total and primary (HO_2) ozone production rates, using box-model results (including measured VOC's) for each data point sampled on the DC-8.

308

309

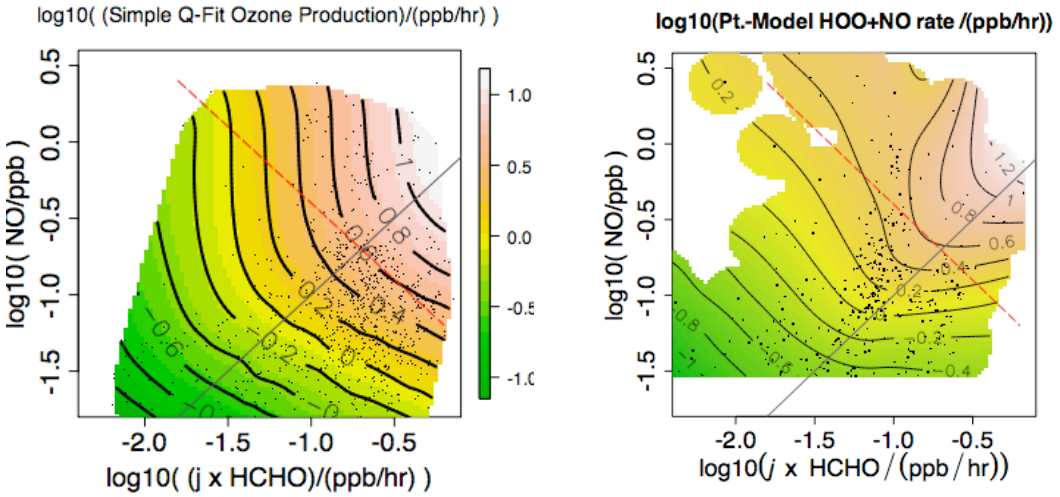

309
310 **A** **B**

Fig. 3. (a) Two-parameter fit for ozone production Q_2 based on an empirical reaction-kinetic model of [HO_2]. 1:1 and 1:-1 lines are as in Figure 1b. Behavior for high NO and low ϕ differs significantly from F_2. (b) Similar two-dimensional relationship derived from point modeling of kinetics, with behavior somewhat intermediate but differing from both F_2 and Q_2 at high ϕ, low ν. Note: Color shadings are not uniform from one contour graph to another.

311
312

Affiliations
(1) Robert B. Chatfield: NASA Ames, Moffett Field, CA, USA Robert.B.Chatfield@nasa.gov
(2) Xinrong Ren, Rosenstiel School, U. Miami, Miami, FL, USA
(3) William H. Brune, Pennsylvania State U., State College, PA, USA
(4) James H. Crawford, NASA Langley, Hampton, VA, USA
(5,1) Robert Esswein, BAER Institute and NASA Ames, Moffett Field CA, USA
(6) Alan Fried, National Center for Atmospheric Research, Boulder, CO, USA
(4) Jennifer R. Olson, NASA Langley, Hampton, VA, USA
(6) Richard E. Shetter, National Center for Atmospheric Research, Boulder, CO, USA